DOI: 10.1002/ange.201106651

Fluid Catalytic Cracking

Integrated Laser and Electron Microscopy Correlates Structure of Fluid Catalytic Cracking Particles to Brønsted Acidity**

*Matthia A. Karreman, Inge L. C. Buurmans, John W. Geus, Alexandra V. Agronskaia, Javier Ruiz-Martínez, Hans C. Gerritsen, and Bert M. Weckhuysen**

Fluid catalytic cracking (FCC) is the main industrial process used worldwide to convert crude oil fractions into fuels and important base chemicals, such as light olefins.[1] This is achieved by using micron-sized spherical catalyst particles of complex composition. Zeolitic material, usually zeolite Y, is the main acidic active cracking ingredient and it is embedded in a matrix consisting of clay, silica, and alumina.

Fluorescence microscopy (FM) experiments made major contributions to the visualization and investigation of active sites within heterogeneous catalyst materials.[2] Confocal FM, for instance, was employed to selectively visualize the active zeolite component within FCC catalyst particles.[3] However, FM has limited spatial resolution and solely reveals fluorescent structures. Electron microscopy (EM), on the other hand, allows for high-resolution imaging of nanometer-sized structural details of the sample without the use of probe molecules.[4] Unlike FM, EM does not enable identification of the active areas in the FCC particles. Therefore, we combine the strengths of both FM and EM in the characterization of FCC particles.

The integrated laser and electron microscope (iLEM) is a novel imaging tool, which was recently introduced in life science research.[5] iLEM combines the strength of FM and transmission electron microscopy (TEM) in one setup. It enables rapid identification of fluorescent domains and subsequent investigation of these regions with superior resolution. Here, we report on the first application of iLEM in material science and, more specifically, in the area of heterogeneous catalysis. FCC catalyst particles[6] were investigated after performing the Brønsted acid catalyzed oligomerization reaction of 4-fluorostyrene. Previous confocal FM and UV/Vis microspectroscopy studies showed that fluorescent products of such Brønsted acid catalyzed probe reactions are mainly formed within the Brønsted acidic zeolite component.[7] By employing iLEM, the Brønsted acidity (measured by fluorescence intensity) can be directly correlated to the structural organization of the FCC particles. The approach and the iLEM setup are schematically shown in Figure 1.

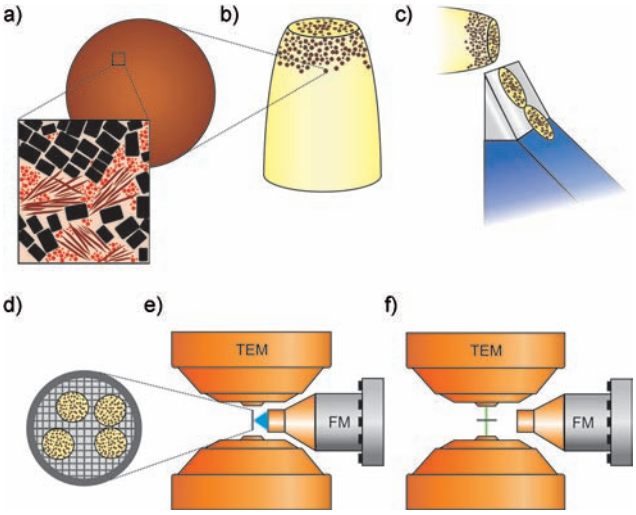

Figure 1. The experimental approach and the iLEM setup. a) An FCC catalyst particle and a structural detail containing zeolite Y crystallites (black, rectangles), clay platelets (brown, elongated structures), and amorphous material (red, dotted structures) are displayed. b) The FCC particles are embedded in a resin (yellow) after reaction with 4-fluorostyrene at 423 K. c) 90 nm thin sections of the FCC material are obtained and d) placed on a TEM grid. Panels (e) and (f) show a schematic inside view of a part of the iLEM. The iLEM consists of a custom-designed laser scanning FM mounted on a side port of a TEM. A detail of the FM is displayed, on the right, positioned in between the two poles of the objective lens of the TEM. The laser beam is perpendicular to the path of the electron beam. e) For FM imaging of the sliced particles, the grid is rotated 90° to face the laser beam (in blue). f) To allow for TEM imaging, the FM is partially retracted and the grid is tilted to its 0° position.

The FM and TEM images were correlated to obtain more insight into the fluorescence intensity and local structure within the catalyst particles. Areas of the FCC particle showing bright and dim fluorescence in the FM (Figure 2a) were relocated in the TEM (Figure 2b). Subsequently, the

[*] M. A. Karreman,[+] I. L. C. Buurmans,[+] Dr. A. V. Agronskaia, Dr. J. Ruiz-Martínez, Prof. Dr. H. C. Gerritsen, Prof. Dr. B. M. Weckhuysen
Debye Institute for Nanomaterials Science
Faculty of Science, Utrecht University
Universiteitsweg 99, 3584 CG Utrecht (The Netherlands)
E-mail: b.m.weckhuysen@uu.nl
Prof. Dr. J. W. Geus
Biomolecular Imaging, Institute of Biomembranes
Faculty of Sciences, Utrecht University
Padualaan 8, 3584 CH Utrecht (The Netherlands)
[+] These authors contributed equally to this work.

[**] We thank H. C. van der Meij and G. C. van Leerdam (Akzo Nobel Chemicals bv, The Netherlands) for ultramicrotomy procedures and C. T. Johnston (Purdue University, USA) and R. A. Schoonheydt (KU Leuven, Belgium) for fruitful discussions. B.M.W. thanks Albemarle Catalysts for financial support and for providing the FCC catalysts, as well as ACTS-Aspect for a grant. M.A.K. acknowledges the Technology Foundation "Stichting Technologische Wetenschappen" for funding.

Supporting information for this article is available on the WWW under http://dx.doi.org/10.1002/anie.201106651.

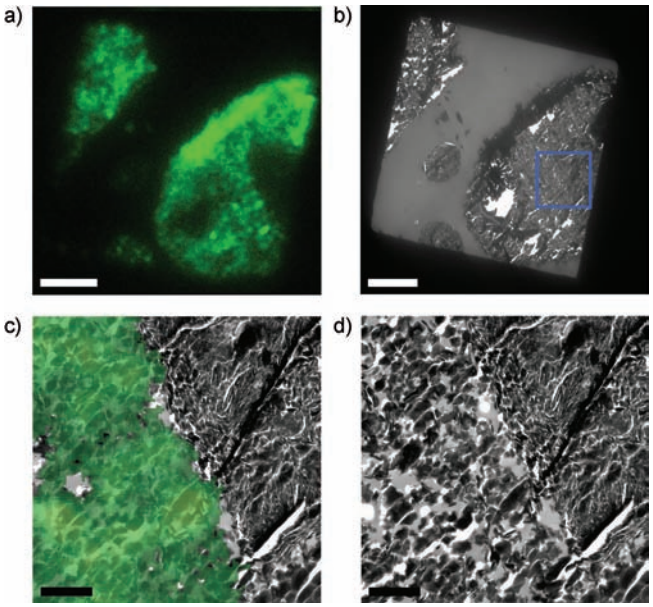

Figure 2. iLEM analysis of a sectioned FCC catalyst particle. a) FM image, b) TEM image, taken from the same region. The area highlighted in (b) with the blue square is shown at higher magnification in panel (c), an overlay of a TEM and FM image, and panel (d), only the TEM image. Scale bars represent 10 μm in (a) and (b) and 2 μm in (c) and (d).

structure of these areas was investigated in detail (Figure 2c,d). A pictorial representation of the different structural features encountered in the TEM images is shown in the inset of Figure 1a. We set out to investigate the relationship between structure and Brønsted acidity of the regions within the FCC particles. Hereto, a statistical analysis was performed on 84 different regions in FCC particles imaged with the iLEM. Two distinct structural types were found in the TEM images: type I, mainly composed of electron dense angular structures, and type II, characterized by a more tightly packed appearance filled with platelet structures and amorphous-looking granular material. Furthermore, an intermediate type I/II was identified, which shows a mixture of structural elements of both subtypes (Figure 3a–c).

TEM images of the different regions were first sorted into type I, I/II, and II, based on their structural characteristics alone. Next, the fluorescence intensity for each of the regions was measured. Areas, in which bright fluorescence was observed, always belonged to type I or I/II. Likewise, the areas showing the lowest fluorescence intensity were always classified as type II or I/II (Figure 3d). This shows that structurally different areas within FCC particles display distinct fluorescence levels. Types I and II are different in both structure and fluorescence intensity, whereas type I/II reveals a mixture of type I and II in terms of local structure and variations in fluorescence intensity. Statistically, there is a significant difference between the fluorescence intensities measured for type I, I/II, and II ($p \ll 0.05$, t-test).

Once a correlation between structural type and fluorescence intensity level was established, the next step was to identify the components, which are characteristic for each type. As exemplified in Figure 3a, type I contains almost exclusively structures with dimensions of a few hundred nanometers that display a very strong structural resemblance to pure zeolite Y crystals (Figure 3e). Electron diffraction patterns of type I areas confirm that these structures correspond to zeolite Y. The high fluorescence intensities in type I areas can therefore be explained by the presence of Brønsted acidity within the zeolite component, forming the fluorescent products.

In the type II areas platelike components, assumed to be clay particles, and an amorphous material were recognized (Figure 3c). To be able to structurally identify the matrix components, a zeolite Y lacking reference FCC particle was imaged which solely consisted of clay, silica, and alumina (Figure 3f). A strong structural resemblance was found between TEM images of the components in these FCC particles and the type II regions. Electron diffraction confirmed that the observed platelike structures within the catalyst particles are indeed a clay material. These results show that the type II areas are mainly composed of matrix material. The low fluorescence signal observed in these areas is therefore expected, since the matrix components do not display significant Brønsted acidity.

In summary, we have found that the type I areas mainly consist of zeolite Y and type II mostly of matrix material. Since the zeolite and the matrix material appear to cluster in different areas, it can be concluded that they are not homogeneously distributed within the FCC particles.

The iLEM was further employed to investigate the changes in structure and fluorescence of the FCC particles following hydrothermal deactivation with steam. Steam deactivation also occurs in industrial FCC units and leads to structural and chemical changes of the different FCC catalyst components. Zeolite structures can be partially damaged by steam because of the extraction of Al atoms from the framework. New extra-framework Al species are created and the amount of Brønsted acid sites in the zeolitic material is lowered. This is reflected in a decrease in the reactivity towards the formation of fluorescent products, as previously described.[8] In agreement with this loss in Brønsted acidity, iLEM fluorescence microscopy images of steamed FCC particles showed much lower fluorescence intensity compared to fresh FCC particles (Figure 4a,b). The steam treatment also affected the structure of the zeolite crystals (Figure 4c,d): a large fraction of the crystals appeared to be damaged and more porous. Electron diffraction of steamed FCC particles revealed that in addition to the diffraction maxima of zeolite Y (small black dots in Figure 4e) additional diffraction rings appeared (black rings in Figure 4e). These diffraction rings confirm the presence of small γ-Al_2O_3 crystallites, which are formed upon zeolite de-alumination. Structural characterization of the steamed catalyst particles furthermore showed that although zeolite crystallites and amorphous material were still present, the large regions of clay regularly found in the fresh FCC particles were lost.

In conclusion, iLEM allowed for the detailed characterization of FCC catalyst particles. The active component could be identified based on fluorescent signal and further analyzed at high resolution with TEM. In the FCC particles not only the structure of the active component was identified as

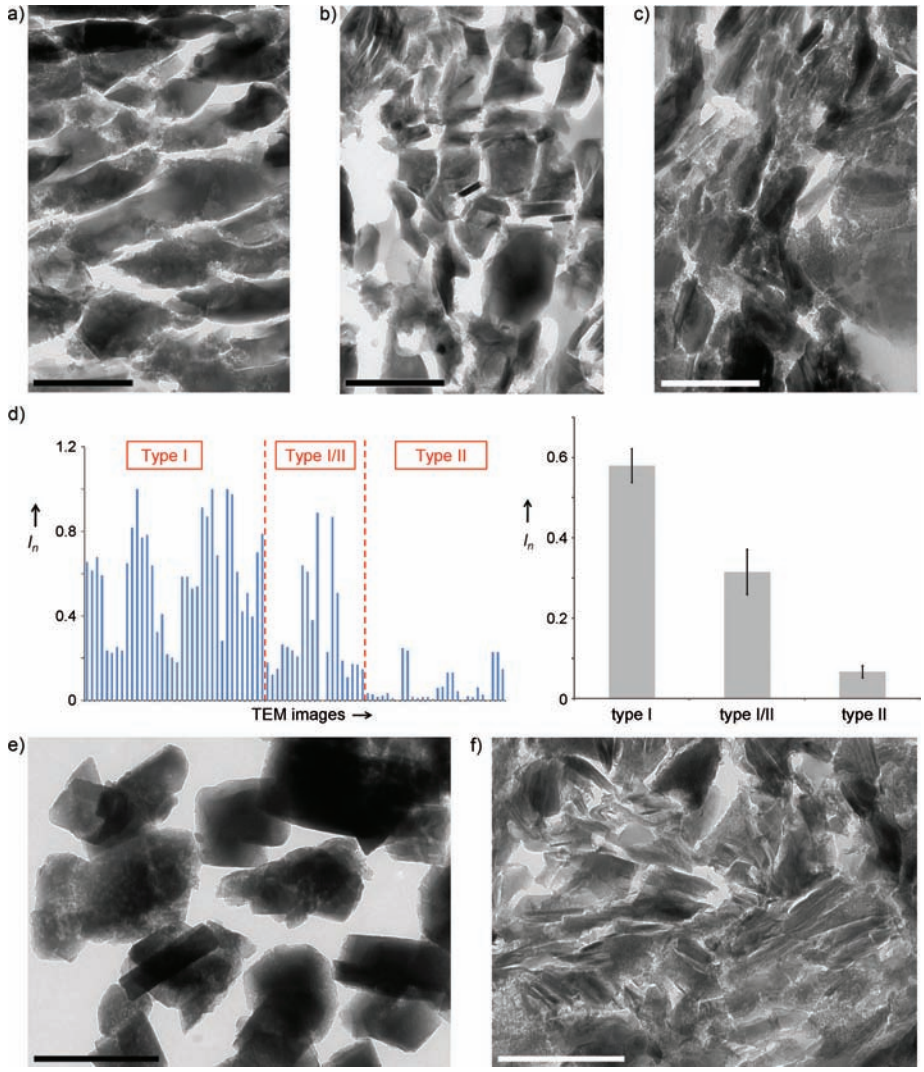

Figure 3. Representative TEM images from the FCC catalyst particles: a) type I, b) type I/II, and c) type II. d) The TEM images of the 84 investigated areas of different catalyst particles were ordered into the three structural types and the FM intensity was measured. The left graph indicates the normalized fluorescence intensity (I_n) measured for each area (TEM images). The graph on the right shows the average normalized fluorescence intensities (I_n) of all images sorted into the three structural subtypes and their standard errors (error bars). e) Reference TEM images of separate zeolite Y crystallites and f) sections of catalyst particles with only clay platelets and amorphous components. Scale bars all represent 500 nm.

zeolite Y, but also the matrix structure was visualized. Previous studies with confocal FM in combination with the electron diffraction experiments described here corroborate the truthfulness of our novel approach. Moreover, this approach shows sensitivity to changes in activity, structure, and chemical properties of the catalytic material.

Experimental Section

Imaging: The majority of the imaging was performed with the integrated laser and electron microscope (iLEM). The iLEM consists of a Tecnai 12 120 kV TEM (FEI Company) and a custom-designed laser scanning FM mounted on one of its side ports. All TEM images were recorded at 80 kV with a bottom mounted TEMCam-F214 (Tietz video and image processing systems) charge-coupled device (CCD) camera. A 488 nm laser (Bluephoton, Omicron Laserage Laserprodukte GmbH) was used for excitation of the sample and fluorescence was detected by an avalanche photodiode (APD, PerkinElmer) detector after passing through a long-pass 520 nm filter. Operation of the FM of the iLEM is performed by software written in LabView 8.0. The selected area diffraction patterns and Figure 4d were imaged with a field emission gun Tecnai 20 (FEI Company) operating at 200 kV, equipped with a SIS MegaView II CCD camera, and analyzed in iTEM. For image processing Photoshop CS4 was employed. To overlay the fluorescence image and the TEM image the γ-value of the fluorescence image was adjusted. In all figures, the TEM and FM images were scaled for optimal contrast by employing linear adjustments of the levels of the entire image. For additional experimental details please refer to the Supporting Information.

Received: September 19, 2011
Published online: December 23, 2011

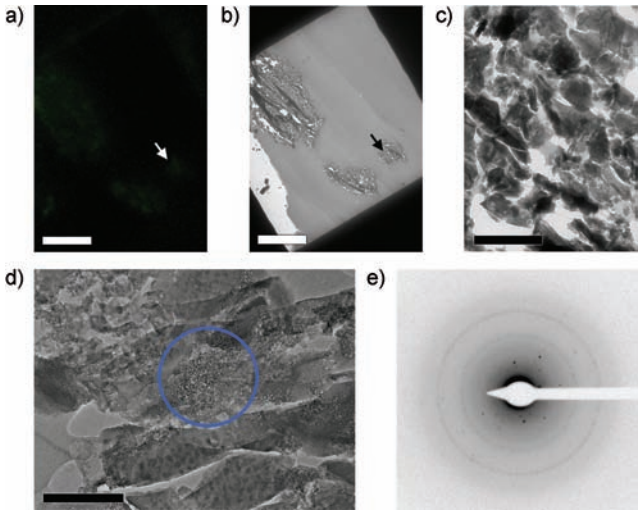

Figure 4. Analysis of FCC catalyst particles after steam deactivation. a) FM image of sectioned steamed FCC particles, the fluorescence intensity is scaled by a factor of six compared to Figure 2a; b) TEM image from the same region. Image (c) shows the area indicated in (a) and (b) with an arrow at high magnification. d) High-magnification TEM image of a detail of a steamed FCC particle. Note the pores in the zeolites and the amorphous material surrounding them. e) The diffraction pattern (inverted) of the region indicated by the blue circle in (d). Here, both diffraction spots characteristic for zeolite Y and diffraction rings corresponding to the presence of small γ-Al_2O_3 crystallites are visible. Scale bars represent 10 μm in (a) and (b), 500 nm in (c), and 200 nm in (d).

Keywords: Brønsted acidity · fluorescence microscopy · heterogeneous catalysis · transmission electron microscopy · zeolites

[1] W. Vermeiren, J.-P. Gilson, *Top. Catal.* **2009**, *52*, 1131 – 1161; H. F. Rase, *Handbook of Commercial Catalysts*, CRC Press, Boca Raton, **2000**; M. Rigutto in *Zeolites and Catalysis: Synthesis Reactions and Applications*, *Vol. 2*, *1 st ed.* (Eds.: J. Čejka, A. Corma, S. I. Zones), Wiley-VCH, Weinheim, **2010**, pp. 547 – 584.

[2] T. Tachikawa, S. Yamashita, T. Majima, *J. Am. Chem. Soc.* **2011**, *133*, 7197 – 7204; G. De Cremer, M. B. J. Roeffaers, E. Bartholomeeusen, K. Lin, P. Dedecker, P. P. Pescarmona, P. A. Jacobs, D. E. De Vos, J. Hofkens, B. F. Sels, *Angew. Chem.* **2010**, *122*, 920 – 923; *Angew. Chem. Int. Ed.* **2010**, *49*, 908 – 911; G. De Cremer, B. F. Sels, D. E. De Vos, J. Hofkens, M. B. J. Roeffaers, *Chem. Soc. Rev.* **2010**, *39*, 4703 – 4717; W. Xu, J. S. Kong, Y. T. E. Yeh, P. Chen, *Nat. Mater.* **2008**, *7*, 992 – 996.

[3] I. L. C. Buurmans, J. Ruiz-Martínez, W. V. Knowles, D. van der Beek, J. A. Bergwerff, E. T. C. Vogt, B. M. Weckhuysen, *Nat. Chem.* **2011**, *3*, 862 – 867.

[4] O. Bayraktar, E. L. Kugler, *Catal. Lett.* **2003**, *90*, 155 – 160; R. A. Beyerlein, G. A. Tamborski, C. L. Marshall, B. L. Meyers, J. B. Hall, B. J. Huggins, *ACS Symp. Ser.* **1991**, *452*, 109 – 143.

[5] A. V. Agronskaia, J. A. Valentijn, L. F. van Driel, C. T. W. M. Schneijdenberg, B. M. Humbel, P. M. P. van Bergen en Henegouwen, A. J. Verkleij, A. J. Koster, H. C. Gerritsen, *J. Struct. Biol.* **2008**, *164*, 183 – 189; M. A. Karreman, A. V. Agronskaia, A. J. Verkleij, F. F. M. Cremers, H. C. Gerritsen, B. M. Humbel, *Biol. Cell* **2009**, *101*, 287 – 299; M. A. Karreman, E. G. van Donselaar, H. C. Gerritsen, C. T. Verrips, A. J. Verkleij, *Traffic* **2011**, *12*, 806 – 814.

[6] The FCC 2 catalyst as described in Ref. [3].

[7] I. L. C. Buurmans, E. A. Pidko, J. M. de Groot, E. Stavitski, R. A. van Santen, B. M. Weckhuysen, *Phys. Chem. Chem. Phys.* **2010**, *12*, 7032 – 7040; I. L. C. Buurmans, J. Ruiz-Martínez, S. L. van Leeuwen, D. van der Beek, J. A. Bergwerff, W. V. Knowles, E. T. C. Vogt, B. M. Weckhuysen, *Chem. Eur. J.* **2011**, DOI: 10.1002/chem.201102949.

[8] L. R. Aramburo, L. Karwacki, P. Cubillas, S. Asahina, D. A. M. de Winter, M. R. Drury, I. L. C. Buurmans, E. Stavitski, D. Mores, M. Daturi, P. Bazin, P. Dumas, F. Thibault-Starzyk, J. A. Post, M. W. Anderson, O. Terasaki, B. M. Weckhuysen, *Chem. Eur. J.* **2011**, *17*, 13773 – 13781.

